

Invariance vs. Robustness of Neural Networks

Sandesh Kamath¹, Amit Deshpande², K V Subrahmanyam¹

¹Chennai Mathematical Institute, Chennai

²Microsoft Research, India

ksandeshk@cmi.ac.in, amitdesh@microsoft.com, kv@cmi.ac.in

Abstract

We study the performance of neural network models on random geometric transformations and adversarial perturbations. Invariance means that the model’s prediction remains unchanged when a geometric transformation is applied to an input. Adversarial robustness means that the model’s prediction remains unchanged after small adversarial perturbations of an input. In this paper, we show a quantitative trade-off between rotation invariance and robustness. We empirically study the following two cases: (a) change in adversarial robustness as we improve only the invariance of equivariant models via training augmentation, (b) change in invariance as we improve only the adversarial robustness using adversarial training. We observe that the rotation invariance of equivariant models (StdCNNs and GCNNs) improves by training augmentation with progressively larger random rotations but while doing so, their adversarial robustness drops progressively, and very significantly on MNIST. We take adversarially trained LeNet and ResNet models which have good L_∞ adversarial robustness on MNIST and CIFAR-10, respectively, and observe that adversarial training with progressively larger perturbations results in a progressive drop in their rotation invariance profiles. Similar to the trade-off between accuracy and robustness known in previous work, we give a theoretical justification for the invariance vs. robustness trade-off observed in our experiments.

1 Introduction

Neural networks achieve state of the art accuracy on several standard datasets used in image classification. However, their performance in the wild depends on how well they can handle natural or non-adversarial transformations of input seen in real-world data as well as known deliberate, adversarial attacks created to fool the model.

Natural or non-adversarial transformations seen in real-world images include translations, rotations, and scaling. Convolutional Neural Networks (CNNs) are translation-invariant or shift-invariant by design. Invariance to other

symmetries, and especially rotations, have received much attention recently, e.g., Harmonic Networks (H-Nets) [Worrall *et al.*, 2016], cyclic slicing and pooling [Dieleman *et al.*, 2016], Transformation-Invariant Pooling (TI-Pooling) [Laptev *et al.*, 2016], Group-equivariant Convolutional Neural Networks (GCNNs) [Cohen and Welling, 2016], Steerable CNNs [Cohen and Welling, 2017], Deep Rotation Equivariant Networks (DREN) [Li *et al.*, 2017], Rotation Equivariant Vector Field Networks (RotEqNet) [Marcos *et al.*, 2017], and Polar Transformer Networks (PTN) [Esteves *et al.*, 2018]. For a given symmetry group G , a G -equivariant network learns a representation or feature map at every intermediate layer such that any transformation $g \in G$ applied to an input corresponds to an equivalent transformation of its representations. Any model can improve its invariance to a given group of symmetries through sufficient training augmentation. Equivariant models use efficient weight sharing [Kondor and Trivedi, 2018] and require smaller sample complexity to achieve better invariance. Equivariant models such as CNNs and GCNNs too generalize well to progressively larger random rotations, but only when their training data is augmented similarly.

Adversarial attacks on neural network models are certain, deliberate changes to inputs that fool a highly accurate model but are unlikely to fool humans. Given any neural network model, Szegedy *et al.* [2013] show how to change the pixel values of images only slightly so that the change is almost imperceptible to human eye but makes highly accurate models misclassify. They find these adversarial pixel-wise perturbations of small magnitude by maximizing the prediction error of a given model using box-constrained L-BFGS. Goodfellow *et al.* [2015] propose Fast Gradient Sign Method (FGSM) that adversarially perturbs x to $x' = x + \epsilon \text{sign}(\nabla_x J(\theta, x, y))$. Here $J(\theta, x, y)$ is the loss function used to train the network, x is the input and y is the target label and θ are the model parameters. Goodfellow *et al.* [2015] propose adversarial training, or training augmented with points (x', y) , as a way to improve adversarial robustness of a model.

Subsequent work introduced multi-step variants of FGSM. Kurakin *et al.* [2017] use an iterative method to produce an attack vector. Madry *et al.* [2018] proposed the Projected Gradient Descent (PGD) attack. Given any model, these attacks produce adversarial perturbation for every test image x from a small ℓ_∞ -ball around it, namely, each pixel value

x_i is perturbed within $[x_i - \epsilon, x_i + \epsilon]$. PGD attack does so by solving an inner optimization by projected gradient descent over ℓ_∞ -ball of radius ϵ around x , to approximate the optimal perturbation. Adversarial training with PGD perturbations improves the adversarial robustness of models and it is one of the best known defenses to make models robust to perturbations of bounded ℓ_∞ norm on MNIST and CIFAR-10 datasets [Madry *et al.*, 2018; Athalye *et al.*, 2018].

Recent work has looked at simultaneous robustness to multiple adversarial attacks. Engstrom *et al.* [2019] show that adversarial training with PGD makes CNNs robust against perturbations of bounded ℓ_∞ norm but an adversarially chosen combination of a small rotation and a translation can nevertheless still fool these models. In Schott *et al.* [2019], the authors show that PGD adversarial training is a good defense against perturbations of bounded ℓ_∞ norm but can be broken with adversarial perturbations of small ℓ_0 or ℓ_2 norm that are also imperceptible to humans or have little semantic meaning for humans. Schott *et al.* [2019] show how to build models for MNIST dataset that are simultaneously robust to perturbations of small ℓ_0 , ℓ_2 and ℓ_∞ norms.

1.1 Problem formulation and our results

Let f be a neural network classifier trained on a training set of labeled images. The accuracy of f is the fraction of test inputs x for which the predicted label $f(x)$ matches the true label y . Similarly, for a given adversarial attack \mathcal{A} , the *fooling rate* of \mathcal{A} on f is the fraction of test inputs $x + \mathcal{A}(x)$ for which $f(x + \mathcal{A}(x)) \neq f(x)$. For a given transformation T of the image space, f is said to be T -invariant if the predicted label remains unchanged after the transformation T for all inputs, i.e., $f(Tx) = f(x)$, for all inputs x . If f is T -invariant and $f(x + \mathcal{A}(x)) \neq f(x)$, for some input x and its adversarial perturbation $\mathcal{A}(x)$ with $\|\mathcal{A}(x)\|_p \leq \epsilon$, then by invariance $f(Tx + T\mathcal{A}(x)) = f(x + \mathcal{A}(x)) \neq (f(x) = f(Tx))$. Let T be a translation, rotation, or, more generally, a permutation of coordinates as considered by Tramer and Boneh [2019]. We have $\|T\mathcal{A}(x)\|_p = \|\mathcal{A}(x)\|_p \leq \epsilon$. Hence, $T\mathcal{A}(x)$ is an adversarial perturbation for input Tx of small ℓ_p norm. When a change of variables maps x to Tx by a permutation of coordinates, then the gradient and T operators can be swapped. In other words, $\text{grad}(f)$ at Tx is the same as T applied to $\text{grad}(f)$ at x . This gives a 1-1 correspondence between FGSM (and PGD) perturbations of x and Tx , respectively, with ℓ_p norm at most ϵ . As a corollary, the ℓ_p fooling rate for any T -invariant classifier f on the transformed data $\{Tx : x \in \mathcal{X}\}$ must be equal to its ℓ_p fooling rate on the original data \mathcal{X} .

A subtlety kicks in when f is not truly invariant, that is, $f(Tx) = f(x)$, for most inputs x but not all x . Define the *rate of invariance* of a classifier f to a transformation T as the fraction of test images whose predicted labels remain unchanged when T is applied to x , i.e., $f(Tx) = f(x)$. For a class of transformations, e.g., rotations upto degree $[-\theta^\circ, +\theta^\circ]$, we define the *rate of invariance* as the average rate of invariance over transformations T in this class. The rate of invariance is 100% if the model f is truly invariant. When f is not truly invariant, the interplay between the invariance under transformations and robustness under adver-

sarial perturbations of small ℓ_p -norm is subtle. *This interplay is exactly what we investigate.*

In this paper, we study neural network models and the simultaneous interplay between their rate of invariance for random rotations between $[-\theta^\circ, +\theta^\circ]$, and their adversarial robustness to pixel-wise perturbations of ℓ_∞ norm at most ϵ . Measuring the robustness of a model to adversarial perturbations of ℓ_p norm at most ϵ is NP-hard [Katz *et al.*, 2017; Sinha *et al.*, 2018]. Athalye *et al.* [2018] compare most of the known adversarial attacks and argue that PGD is among the strongest. Therefore, we use a models accuracy on test data adversarially perturbed using PGD as a proxy for its adversarial robustness.

Unlike previous studies by Engstrom *et al.* [2019] and Tramer and Boneh [2019], we do not fix the magnitude of pixel-wise adversarial perturbations (e.g., say $\epsilon = 0.3$), nor do we limit ourselves to small rotations up to $\pm 30^\circ$. Another important difference is we consider random rotations instead of adversarial rotations. We compute the rate of invariance of a given model on inputs rotated by a random angle between $[-\theta^\circ, +\theta^\circ]$, for θ varying in the range $[0, 180]$. Similarly, we normalize the underlying dataset, and compute the accuracy of a given model on test inputs adversarially perturbed using PGD attack of ℓ_∞ norm at most ϵ , for ϵ varying in the range $[0, 1]$.

We empirically study the following: (a) change in ℓ_∞ adversarial robustness as we improve only the rate of rotation invariance using training augmentation with progressively larger rotations, (b) change in invariance as we improve only adversarial robustness using PGD adversarial training with progressively larger ℓ_∞ -norm of pixel-wise perturbations.

We study equivariant models, StdCNNs and GCNNs, as well as LeNet and ResNet models used by Madry *et al.* [2018]. Equivariant models, especially GCNNs, when trained with random rotation augmentations come very close to being truly rotation invariant [Cohen and Welling, 2016; Cohen and Welling, 2017; Cohen and Weiler, 2018]. StdCNNs are translation-equivariant by design and GCNNs are rotation-equivariant by design through clever weight sharing [Kondor and Trivedi, 2018]. However, these models do not have high rate of invariance if their training data is not sufficiently augmented. This appears to be folklore so we do not elaborate on this. LeNet and ResNet models adversarially trained with PGD are among the best known ℓ_∞ adversarially robust models on MNIST and CIFAR-10, respectively, as shown by Madry *et al.* [2018], and reconfirmed by Athalye *et al.* [2018]. In other words, equivariant models with training augmentation and PGD-trained LeNet and ResNet models essentially represent the two separate solutions known currently for achieving invariance and adversarial robustness, respectively.

Our two main observations are as follows.

- (i) Equivariant models (StdCNNs and GCNNs) progressively improve their rate of rotation invariance when their training is augmented with progressively larger random rotations but while doing so, their ℓ_∞ adversarial robustness drops progressively. This drop or trade-off is very significant on MNIST.

- (ii) LeNet and ResNet models adversarially trained using progressively larger ℓ_∞ -norm attacks improve their adversarial robustness but while doing so, their rate of invariance to random rotations upto $\pm\theta^\circ$ drops progressively.

We give a theoretical justification for the invariance vs. robustness trade-off observed in our experiments (see Theorem 1) by building upon the ideas in previous work on accuracy vs robustness trade-off [Tsipras *et al.*, 2019; Tramèr and Boneh, 2019].

Related Work. Schott *et al.* [2019] study simultaneous robustness to adversarial perturbations of small ℓ_0 , ℓ_2 , and ℓ_∞ -norm. Tramèr and Boneh [2019] show an impossibility result by exhibiting a data distribution where no binary classifier can have substantially better-than-random accuracy simultaneously against both ℓ_∞ and ℓ_1 perturbations. They consider a spatial perturbation that permutes a small number of coordinates of the input to model a combination of a small translation and a small rotation. They also construct a distribution and show that no model can have good accuracy simultaneously against both ℓ_∞ perturbations and spatial perturbations. They empirically validate this claim on MNIST and CIFAR-10 datasets for simultaneous robustness against ℓ_∞ adversarial perturbation and an adversarially chosen combination of translations upto ± 3 pixels and rotations upto $\pm 30^\circ$. Intuitively and theoretically, it has been argued by Tsipras *et al.* [2019] and Tramèr and Boneh [2019] that *small, adversarial pixel-wise perturbations* and *small, adversarial geometric transformations* are essentially dissimilar attacks focusing on different features, due to which a simultaneous solution to both may be inherently difficult. They do not postulate any gradual trade-off between invariance and robustness. They do not consider group-equivariant models such as GCNNs, a natural choice for invariance to geometric transformations.

2 Rotation invariance vs. ℓ_∞ adversarial robustness

In this section, we present our main result about the interplay between rotation invariance and ℓ_∞ adversarial robustness of models on MNIST and CIFAR-10 data. In Subsection 2.1, we take StdCNN and GCNN models (see details in Section 4) and study their rotation invariance and ℓ_∞ adversarial robustness, as we train them with random rotations of progressively larger degree. In Subsection 2.2, we take LeNet and ResNet models [Madry *et al.*, 2018] and study their rotation invariance and ℓ_∞ adversarial robustness, as we do PGD adversarial training with progressively larger ℓ_∞ norms.

We present our experimental results as rotation invariance profiles and adversarial robustness profiles explained below.

Rotation invariance means that the predicted labels of an image and any of its rotations should be the same. Since most datasets are centered, we restrict our attention to rotations about the center of each image. We quantify rotation invariance by measuring the rate of invariance or the fraction of test images whose predicted label remains the same after rotation by a random angle between $[-\theta^\circ, \theta^\circ]$. As θ varies from 0 to 180, we plot the rate of invariance. We call this the *rotation invariance profile* of a given model.

Adversarial robustness means that the predicted labels of an image and its adversarial perturbation should be the same. We quantify the ℓ_∞ adversarial robustness of a given model to a fixed adversarial attack (e.g., PGD) and a fixed ℓ_∞ norm $\epsilon \in [0, 1]$ by $(1 - \text{fooling rate})$, i.e., the fraction of test inputs for which their predicted label does not change after adversarial perturbation. We plot this for ϵ varying from 0 to 1. We call this the *robustness profile* of a given model.

Convention used in the legends of our figures. We use the following convention in the legends of some plots. A coloured line labeled A/B indicates that the training data is augmented with random rotations from $[-A^\circ, A^\circ]$ and the test data is augmented with random rotations from $[-B^\circ, B^\circ]$. If A (resp. B) is zero it means the training data (resp. test data) is unrotated. If the model is trained with random rotations from $[-A^\circ, A^\circ]$ and the test data is randomly rotated with varying B to draw the plot, we only mention A and not B , which is self-explanatory.

2.1 Effect of rotation invariance on ℓ_∞ adversarial robustness

For any fixed $\theta \in [0, 180]$, we take an equivariant model, namely, StdCNN or GCNN, and augment its training data by random rotations from $[-\theta^\circ, +\theta^\circ]$. Figure 1(left), Figure 2(left) shows how the robustness profile of StdCNN change on MNIST and CIFAR-10 respectively, as we increase the degree θ used in training augmentation of the model. We use PGD adversarial attack for MNIST and CIFAR-10. Figure 1(right) and Figure 2(right) show the rotation invariance profile of the same models on MNIST, CIFAR-10 respectively.

The black line in Figure 1 (left), shows that the adversarial robustness of a StdCNN which is trained to handle rotations upto ± 180 degrees on MNIST, drops by more than 50%, even when the ϵ budget for PGD attack on unrotated MNIST is only 0.1. The black line in Figure 1 (right), shows this models rotation invariance profile - this model is invariant to larger rotations in the test data. This can be contrasted with the model depicted by the red line - this StdCNN is trained to handle rotations up to 60 degrees. The rotation invariance profile of this model is below that of the model depicted by the black line and so it is not invariant to large rotations. However this model can handle adversarial ℓ_∞ -perturbations up to 0.3 on unrotated data, with an accuracy more than 80% - this can be seen from the red line in Figure 1 (left).

From these plots it is clear that *the rotation invariance of these models improves by training augmentation but at the cost of their adversarial robustness, indicating a trade-off between invariance to rotations and adversarial robustness.* The above observations, of there being a trade-off between handling larger rotations with training augmentation and handling larger adversarial perturbations is seen in GCNNs also. This can be seen from Figures 3 and Figure 4. The plots are very similar to what we observe with StdCNNs.

2.2 Effect of ℓ_∞ adversarial training on rotation invariance

The most common approach to improve adversarial robustness is adversarial training, i.e., training the model on ad-

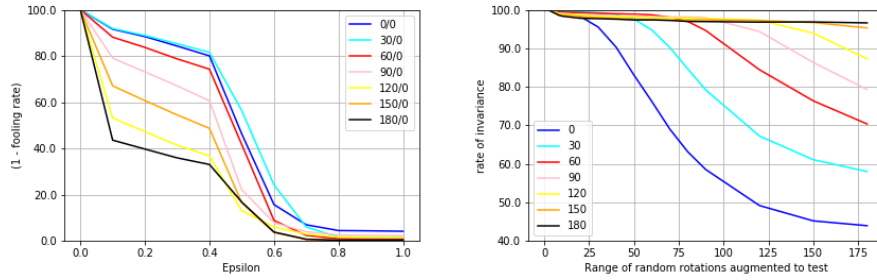


Figure 1: On MNIST, StdCNN trained with varying random rotations in $[-\theta^\circ, \theta^\circ]$ range. (left) Robustness profile, (right) Rotation invariance profile.

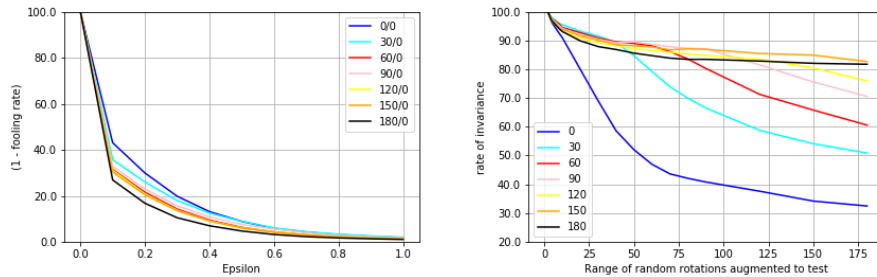


Figure 2: On CIFAR-10, StdCNN/VGG16 trained with varying random rotations in $[-\theta^\circ, \theta^\circ]$ range. (left) Robustness profile, (right) Rotation invariance profile.

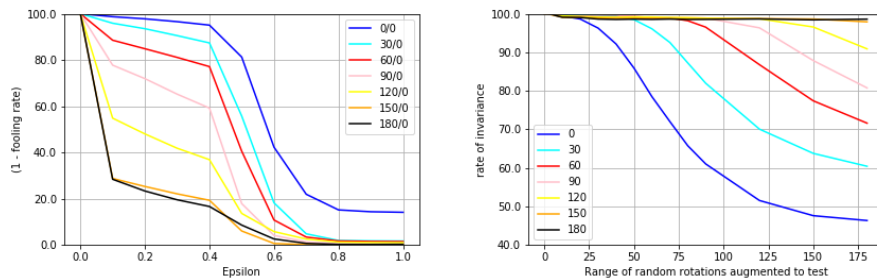


Figure 3: On MNIST, GCNN trained with varying random rotations in $[-\theta^\circ, \theta^\circ]$ range. (left) Robustness profile, (right) Rotation invariance profile.

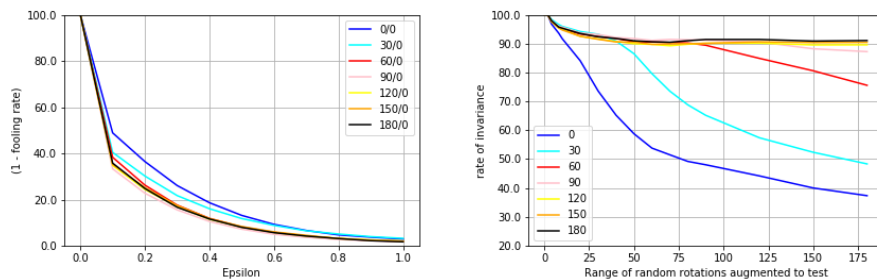


Figure 4: On CIFAR-10, GCNN/VGG16 trained with varying random rotations in $[-\theta^\circ, \theta^\circ]$ range. (left) Robustness profile, (right) Rotation invariance profile.

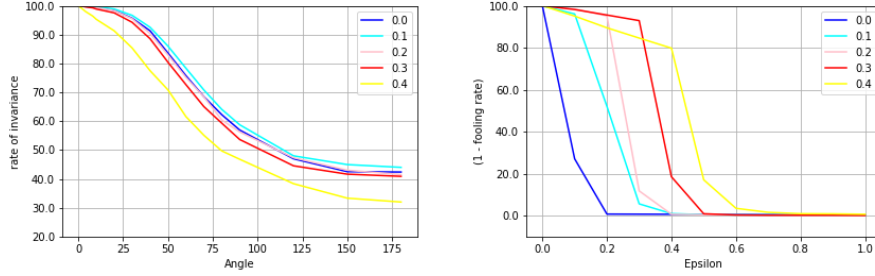


Figure 5: For PGD adversarially trained LeNet based model from [Madry *et al.*, 2018] on MNIST (left) Rotation invariance profile, (right) Robustness profile. Different colored lines represent models adversarially trained with different ℓ_∞ budgets $\epsilon \in [0, 1]$.

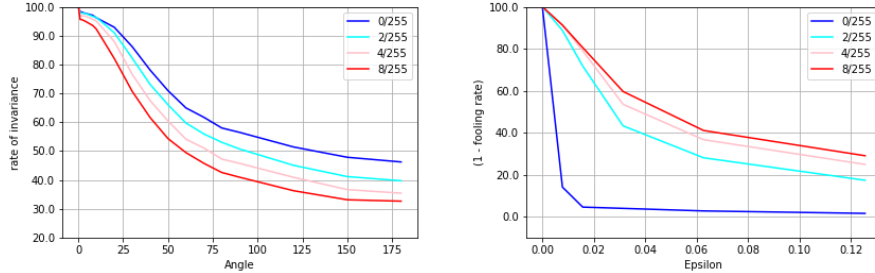


Figure 6: For PGD adversarially trained ResNet based model from [Madry *et al.*, 2018] on CIFAR-10 (left) Rotation invariance profile, (right) Robustness profile. Different colored lines represent models adversarially trained with different ℓ_∞ budgets $\epsilon \in [0, 1]$.

adversarially perturbed training data. Adversarial training with PGD attack is one of the strongest known defenses on MNIST and CIFAR-10 datasets (see [Athalye *et al.*, 2018]).

For any fixed $\epsilon \in [0, 1]$ we adversarially train our models, LeNet and ResNet, as done by Madry *et al.* [2018] with PGD adversarial perturbations with ℓ_∞ budget ϵ . As in Madry *et al.* [2018] we use the LeNet model for MNIST and the ResNet model for CIFAR-10. We then plot their rotation invariance profiles and robustness profiles. Each colored line in Figure 5 and Figure 6 corresponds to a model adversarially trained with a different value of ϵ .

On MNIST, adversarial training with PGD with larger ϵ results in a drop in the invariance profile of LeNet based model - in Figure 5 (left), the yellow line (PGD with $\epsilon = 0.4$) is below the light blue line (PGD with $\epsilon = 0.1$). Similar qualitative drop holds for the ResNet based model too on CIFAR-10, as can be seen from Figure 6 (left). In other words, *adversarial training with progressively larger ϵ leads to the drop in the rate of invariance on the test data.*

To complete this picture we plot the robustness profile curves of the LeNet and ResNet based model for MNIST and CIFAR-10, respectively. It is known that as these models are trained with PGD using larger ϵ budget their adversarial robustness increases. The robustness profile curves of the LeNet model trained with larger PGD budget dominates the robustness profile curve of the same model trained with a smaller PGD budget - the red line in Figure 5 (right), dominates the light blue line. This is true of the ResNet based model too, as can be seen from Figure 6 (right).

3 Invariance vs. robustness trade-off proof

In this section, we give theoretical demonstration of an invariance-vs-robustness trade-off similar to our experiments. We consider an ℓ_∞ adversarial perturbation $\mathcal{A}(x)$ that perturbs the coordinates of any input x by a small value. Observe that rotation by 0° leaves any input x unchanged whereas rotation by 180° keeps the center pixel fixed and makes pairwise swaps for all other pixels radially opposite to each other around the center. We consider a random permutation of coordinates $r(x)$ to mimic picking a uniformly random rotation from $\{0^\circ, 180^\circ\}$. We consider a joint distribution on input-label pairs such that there exists a classifier of high accuracy. However, we prove that no classifier can have high accuracy (w.r.t. true labels) after the random transformation $r(x)$ as well as the adversarial perturbation $\mathcal{A}(x)$, simultaneously. Even though our theorem is about accuracy after $r(x)$ instead of the rate of invariance, and accuracy after $\mathcal{A}(x)$ instead of $(1 - \text{fooling rate})$, these values are close for any classifier that has high accuracy on the original data distribution.

Consider a random input-label pair (X, Y) with $X = (X_0, X_1, \dots, X_{2d})$ taking values in \mathbb{R}^{2d+1} and Y taking values in $\{-1, 1\}$ generated as follows. The class label Y takes value ± 1 with probability $1/2$ each. $X_0 \mid Y = y$ takes value y with probability p and $-y$ with probability $1 - p$, for some $p \geq 1/2$. The remaining coordinates are independent and normally distributed with $X_{2t-1} \mid Y = y$ as $N(3y/\sqrt{d}, 1)$ and $X_{2t} \mid Y = y$ as $N(-3y/\sqrt{d}, 1)$, for $1 \leq t \leq d$. First of all, there exists a classifier $f^*(x) = \text{sign} \left(\sum_{t=1}^d x_{2t-1} \right)$

with high accuracy $\Pr\left(\text{sign}\left(\sum_{i=1}^d X_{2i-1}\right) = Y\right) > 99\%$ for this data distribution. The proof of this follows from the three-sigma rule for normal distributions, and is similar to the equation (4) in Subsection 2.1 of Tsipras et al. [2019].

Let $\mathcal{A}(x)$ denote an adversarial perturbation for (x, y) given by $(\mathcal{A}(x))_0 = 0$, and $(\mathcal{A}(x))_{2t-1} = -6y/\sqrt{d}$, $(\mathcal{A}(x))_{2t} = 6y/\sqrt{d}$, for $1 \leq t \leq d$. Note that $\|\mathcal{A}(x)\|_\infty = 6/\sqrt{d}$, for all $x \in \mathbb{R}^{2d+1}$.

Given any input $x \in \mathbb{R}^{2d+1}$, let $r(x)$ be a random transformation of x that leaves x unchanged as $r(x) = x$ with probability $1/2$, and swaps successive odd-even coordinate-pairs (x_{2t-1}, x_{2t}) for $1 \leq t \leq d$ to get $(x_0, x_2, x_1, \dots, x_{2d}, x_{2d-1})$, with probability $1/2$.

Theorem 1. *Given input distributions defined above with $1/2 \leq p < 1 - \delta$, for any classifier $f : \mathbb{R}^{2d+1} \rightarrow \{-1, 1\}$, both $\Pr(f(r(X)) = Y)$ and $\Pr(f(X + \mathcal{A}(X)) = Y)$ cannot be more than $1 - \delta$ simultaneously.*

Proof. The random transformation $r(X)$ leaves X unchanged with probability $1/2$ but with the remaining $1/2$ probability, it makes the data distribution of $r(X)$ the same as $X + \mathcal{A}(X)$. Thus,

$$\begin{aligned} \Pr(f(r(X)) = Y) \\ = \frac{1}{2} \Pr(f(X) = Y) + \frac{1}{2} \Pr(f(X + \mathcal{A}(X)) = Y), \end{aligned}$$

where the LHS probability is over r, X, Y while the RHS probabilities are only over X, Y . Let G_y denote $(X_1, \dots, X_{2d}) \mid Y = y$. The adversarial perturbation $X + \mathcal{A}(X)$ turns G_y into G_{-y} .

$$\begin{aligned} \Pr(f(X + \mathcal{A}(X)) \neq Y) \\ = \frac{1}{2} \sum_{y \in \{-1, 1\}} \Pr(f((X_0, G_{-y})) = -y) \\ = \frac{1}{2} \left\{ \sum_{y \in \{-1, 1\}} p \Pr(f((y, G_{-y})) = -y) \right. \\ \quad \left. + (1-p) \Pr(f((-y, G_{-y})) = -y) \right\} \\ \geq \frac{1-p}{2p} \left\{ \sum_{y \in \{-1, 1\}} (1-p) \Pr(f((y, G_{-y})) = -y) \right. \\ \quad \left. + p \Pr(f((-y, G_{-y})) = -y) \right\} \\ = \frac{1-p}{2p} \left\{ \sum_{y \in \{-1, 1\}} (1-p) \Pr(f((-y, G_y)) = y) \right. \\ \quad \left. + p \Pr(f((y, G_y)) = y) \right\} \\ = \frac{1-p}{p} \Pr(f(X) = Y). \end{aligned}$$

Plugging this in the above expression of $\Pr(f(r(X)) = Y)$ we get

$$\begin{aligned} \Pr(f(r(X)) = Y) + \frac{2p-1}{2(1-p)} \Pr(f(X + \mathcal{A}(X)) = Y) \\ \leq \frac{p}{2(1-p)}. \end{aligned}$$

Standard CNN	GCNN
Conv(10,3,3) + Relu	P4ConvZ2(10,3,3) + Relu
Conv(10,3,3) + Relu	P4ConvP4(10,3,3) + Relu
Max Pooling(2,2)	Group Spatial Max Pooling(2,2)
Conv(20,3,3) + Relu	P4ConvP4(20,3,3) + Relu
Conv(20,3,3) + Relu	P4ConvP4(20,3,3) + Relu
Max Pooling(2,2)	Group Spatial Max Pooling(2,2)
FC(50) + Relu	FC(50) + Relu
Dropout(0.5)	Dropout(0.5)
FC(10) + Softmax	FC(10) + Softmax

Table 1: Architectures used for the MNIST experiments

If both $\Pr(f(r(X)) = Y)$ and $\Pr(f(X + \mathcal{A}(X)) = Y)$ are at least $1 - \delta$, then the above inequality implies $1 - \delta \leq p$. Thus, if $p < 1 - \delta$, we get a contradiction. \square

4 Details of experiments

All experiments performed on neural network-based models were done using MNIST and CIFAR-10 datasets with appropriate augmentations applied to the train/validation/test set.

Data sets. MNIST dataset consists of 70,000 images of 28×28 size, divided into 10 classes. 55,000 used for training, 5,000 for validation and 10,000 for testing. CIFAR-10 dataset consists of 60,000 images of 32×32 size, divided into 10 classes. 40,000 used for training, 10,000 for validation and 10,000 for testing.

Equivariant Model Architectures. For the MNIST based experiments we use the network architecture of GCNN as given in Cohen and Welling [2016]. The StdCNN architecture is similar to the GCNN except that the operations are as per CNNs. Refer to Table 1 for details. For the CIFAR-10 based experiments we use the VGG16 architecture as given in Simonyan and Zisserman [2014] and its GCNN equivalent is obtained replacing the various layer operations with equivalent GCNN operations as given in Cohen and Welling [2016]. This is similar to how we obtained a GCNN architecture from StdCNN for the MNIST based experiments. Input training data was augmented with random cropping and random horizontal flips.

Adversarially Robust Model Architectures. For the adversarial training experiments we used the LeNet based architecture for MNIST and the ResNet architecture for CIFAR-10. Both these models are exactly as given in Madry et al. [2018].

5 Conclusion

We observe that as equivariant models (StdCNNs and GCNNs) are trained with progressively larger rotations their rotation invariance improves but at the cost of their adversarial robustness. Adversarial training with perturbations of progressively increasing norms improves the robustness of LeNet and ResNet models, but with a resulting drop in their rate of invariance. We give a theoretical justification for the invariance-vs-robustness trade-off observed in our experiments.

References

- [Athalye *et al.*, 2018] Anish Athalye, Nicholas Carlini, and David Wagner. Obfuscated gradients give a false sense of security: Circumventing defenses to adversarial examples. In *Proceedings of the 35th International Conference on Machine Learning, ICML 2018*, July 2018.
- [Cohen and Weiler, 2018] Mario Cohen, Taco S. Geiger and Maurice Weiler. A general theory of equivariant cnns on homogeneous spaces. *CoRR*, abs/1811.02017, 2018.
- [Cohen and Welling, 2016] Taco S. Cohen and Max Welling. Group equivariant convolutional networks. In *Proceedings of the International Conference on Machine Learning (ICML)*, 2016.
- [Cohen and Welling, 2017] Taco S. Cohen and Max Welling. Steerable CNNs. In *International Conference on Learning Representations*, 2017.
- [Dieleman *et al.*, 2016] Sander Dieleman, Jeffrey De Fauw, and Koray Kavukcuoglu. Exploiting cyclic symmetry in convolutional neural networks. In *Proceedings of the International Conference on Machine Learning (ICML)*, 2016.
- [Engstrom *et al.*, 2019] Logan Engstrom, Brandon Tran, Dimitris Tsipras, Ludwig Schmidt, and Aleksander Madry. Exploring the landscape of spatial robustness. In *ICML*, 2019.
- [Esteves *et al.*, 2018] Carlos Esteves, Christine Allen-Blanchette, Xiaowei Zhou, and Kostas Daniilidis. Polar transformer networks. In *International Conference on Learning Representations*, 2018.
- [Goodfellow *et al.*, 2015] Ian J. Goodfellow, Jonathon Shlens, and Christian Szegedy. Explaining and harnessing adversarial examples. In *International Conference on Learning Representations*, 2015.
- [Katz *et al.*, 2017] Guy Katz, Clark W. Barrett, David L. Dill, Kyle Julian, and Mykel J. Kochenderfer. Reluplex: An efficient smt solver for verifying deep neural networks. In *CAV*, 2017.
- [Kondor and Trivedi, 2018] Risi Kondor and Shubhendu Trivedi. On the generalization of equivariance and convolution in neural networks to the action of compact groups. In *Proceedings of the International Conference on Machine Learning (ICML)*, 2018.
- [Kurakin *et al.*, 2017] Alexey Kurakin, Ian Goodfellow, and Samy Bengio. Adversarial examples in the physical world. *arXiv preprint arXiv:1607.02533*, 2017.
- [Laptev *et al.*, 2016] Dmitry Laptev, Nikolay Savinov, Joachim M. Buhmann, and Marc Pollefeys. TI-pooling: transformation-invariant pooling for feature learning in convolutional neural networks. In *Proceedings of the IEEE Conference on Computer Vision and Pattern Recognition*, pages 289–297, 2016.
- [Li *et al.*, 2017] Junying Li, Zichen Yang, Haifeng Liu, and Deng Cai. Deep rotation equivariant network. *arXiv preprint arXiv:1705.08623*, 2017.
- [Madry *et al.*, 2018] Aleksander Madry, Aleksandar A Makelov, Ludwig Schmidt, Dimitris Tsipras, and Adrian Vladu. Towards deep learning models resistant to adversarial attacks. In *International Conference on Learning Representations*, 2018.
- [Marcos *et al.*, 2017] Diego Marcos, Michele Volpi, Nikos Komodakis, and Devis Tuia. Rotation equivariant vector field networks. In *International Conference on Computer Vision*, 2017.
- [Schott *et al.*, 2019] Lukas Schott, Jonas Rauber, Matthias Bethge, and Wieland Brendel. Towards the first adversarially robust neural network model on MNIST. In *International Conference on Learning Representations*, 2019.
- [Simonyan and Zisserman, 2014] Karen Simonyan and Andrew Zisserman. Very deep convolutional networks for large-scale image recognition. *CoRR*, abs/1409.1556, 2014.
- [Sinha *et al.*, 2018] Aman Sinha, Hongseok Namkoong, and John C. Duchi. Certifying some distributional robustness with principled adversarial training. In *6th International Conference on Learning Representations, ICLR 2018, Vancouver, BC, Canada, April 30 - May 3, 2018, Conference Track Proceedings*, 2018.
- [Szegedy *et al.*, 2013] Christian Szegedy, Wojciech Zaremba, Ilya Sutskever, Joan Bruna, Dumitru Erhan, Ian J. Goodfellow, and Rob Fergus. Intriguing properties of neural networks. *arXiv preprint arXiv:1312.6199*, 2013.
- [Tramèr and Boneh, 2019] Florian Tramèr and Dan Boneh. Adversarial training and robustness for multiple perturbations. *CoRR*, abs/1904.13000, 2019.
- [Tsipras *et al.*, 2019] Dimitris Tsipras, Shibani Santurkar, Logan Engstrom, Alexander Turner, and Aleksander Madry. Robustness may be at odds with accuracy. In *International Conference on Learning Representations*, 2019.
- [Worrall *et al.*, 2016] D. E. Worrall, S. J. Garbin, D. Turmukhambetov, and G. J. Brostow. Harmonic networks: Deep translation and rotation equivariance. *arXiv preprint arXiv:1612.04642*, 2016.